Int. J. Electrochem. Sci., 7 **(2012)** 7270 - 7282

International Journal of
ELECTROCHEMICAL
SCIENCE
www.electrochemsci.org

Study for the Stability and Corrosion Inhibition of Electrophoretic Deposited Chitosan on Mild Steel Alloy in Acidic Medium

Rasha A. Ahmed [1, 2, 3,*], *R. A. Farghali*[1, 2], *A.M. Fekry*[1]

[1] Chemistry Department, Faculty of Science, Cairo University, Giza 12613, Egypt.
[2] Taif University, Faculty of Science, Chemistry Department, Taif, Hawiya 888, Saudi Arabia
[3] Forensic Chemistry Laboratories, Medico Legal Department, Ministry of Justice, Cairo, Egypt
[*]E-mail: rashaauf@yahoo.com

Received: 3 July 2012 / *Accepted:* 15 July 2012 / *Published:* 1 August 2012

Electrophoretic deposition (EPD) of chitosan (CS) on mild steel substrates was done from a chitosan–acetic acid solution. To increase the protective ability of chitosan coating, the coated samples were immersed in glutaraldehyde solution for 5 minutes. The electrophoretic deposition (EPD) of chitosan on mild steel substrates was investigated by FTIR, scanning electron microscopy, potentiodynamic polarization measurements, and electrochemical impedance spectroscopy (EIS). The results of EIS showed that the resistance (R_t) or film stability increases with increasing immersion time in 0.5 M H_2SO_4 solution indicating a decrease in corrosion rate of the tested alloy with time. EIS measurements under open-circuit conditions confirmed well polarization results. CS showed very good inhibition efficiency (IE) in 0.5 M sulphuric acid solution reaches to 98.1%. The method enabled the formation of adherent, protective and uniform coatings.

Keywords: Chitosan; EIS; Polarization; SEM; Mild steel.

1. INTRODUCTION

Acidic solutions are commonly used in the chemical industry; however, it leads to aggressive corrosion of the metallic surface. The addition of inhibitors affects well on the metallic surface and protects it against an acid attack. Many studies using organic inhibitors have been reported [1-7]. The inhibitor adsorption mode is strictly affected by the inhibitor structure. Most acid inhibitors are organic compounds containing oxygen, nitrogen and/or sulfur. These compounds are adsorbed on the metallic surface blocking the active corrosion sites. Although the most effective and efficient organic inhibitors are compounds that have π bonds, the biological toxicity of these products, especially organic

phosphate, is documented especially about their environmental harmful characteristics [8,9]. From the standpoint of safety, the development of non-toxic and effective inhibitors is considered more important and desirable.

Chitosan (CS), which is derived from the polysaccharide chitin, is well known as a low cost, renewable marine polymer because the source of chitin comes from the structural components of the shells of crustaceans, such as shrimps, lobsters, and crabs [10]; it is the most plentiful natural polymer next to cellulose. CS is produced at an estimated amount of one billion tons per year [11]. The molecular structure of CS is represented by a beta $1\rightarrow4$ linked linear biopolymer consisting of ~80% poly(d-glucosamine) and ~20% poly (*N*-acetyl-d-glucosamine). When CS was dissolved in an aqueous medium at pH<6.5, this biopolymer becomes a linear polybase electrolyte having a highly positive (C) charge density because it includes an amine group [12]. Such a cationic property together with its biocompatability was the reason why CS is widely used in biomedical applications, e.g., a bacteriostatic agent, a flocculating agent, a drug delivery vehicle, an immobilization and encapsulation agent of toxic heavy metals, and also cosmetics. In addition, a tough, flexible CS film can be fabricated by depositing CS-dissolved aqueous solution on the substrate surfaces and then allowing it to dry. This film had a high potential for use as contact lenses and wound dressings. Thus, it seemed worthwhile to assess the usefulness of the non-toxic CS biopolymer as an environmentally green water-based coating to protect metals against corrosion.

Electrophoretic deposition (EPD) is a convenient method to fabricate a great variety of ceramic, polymer and composite coatings for biomedical applications [13]. EPD is a colloidal process in which charged particles or polymer macromolecules in suspension move towards an electrode under the influence of an electrical field. The equipment needed for this process is simple and the coating characteristics can be easily adjusted by the processing parameters [14, 15]. Other advantages are the possibility of depositing materials at room temperature, being possible to achieve also homogeneous coatings with high purity and on complex shaped substrates.

The good film forming ability, specific solubility and versatile chemical functionalization of chitosan make it a promising candidate for "green" protective coatings. The aim of this work is to examine chitosan, which is a good film former, as a corrosion protective coating for mild steel substrate in 0.5M H_2SO_4. In this respect the electrochemical reactivity and passivation behavior of mild steel coated by chitosan CS was investigated in 0.5M H_2SO_4 acid solution. The preparation of chitosan has been described. Different techniques were employed such as cyclic voltammetry, potentiodynamic polarization, impedance spectroscopy (EIS) and scanning electron microscopy (SEM).

2. EXPERIMENTAL DETAILS

2.1. Chemicals preparation

The chitosan (Fig. 1) with a degree of deacetylation of at least 85% was obtained from Sigma–Aldrich. Glutaraldehyde 25% received from Merck. The chitosan solution was prepared by dissolving

under stirring 0.5 g of the compound in 100 mL of 0.1 M acetic acid at room temperature, until all particles were dissolved. This produced a clear and viscous liquid with a pH of about 4; thereafter the solution was stored in a sealed container.

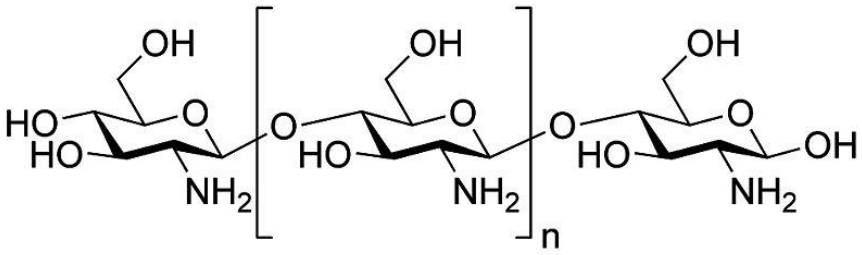

Figure 1. Chitosan structure

EPD was performed using a dilute solution of chitosan. During EPD a constant voltage of 15 V was applied. The deposition was performed at room temperature during 15 min. After EPD, the samples were left to hang dry for 1 hour; a smooth and yellow transparent layer, covering the metal surface, was visually observed. After this, the crosslinker was incorporated by dipping the coated substrate in 10 μL of 2.0% (v/v) of glutaraldehyde solution for 1 min, and left to dry for 24 hours before use.

2.2. Electrode preparation

The tested steel sheet in the present study has area of 0.2814 cm^2. The composition of the steel is as follows (wt%): (0.045%P; 0.3% Si; 0.3% Cr; 0.3–0.65% Mn; 0.14–0.22% C; 0.05% S;0.3% Ni; 0.3% Cu and the remainder Fe)

The mild steel substrates to be modified by chitosan films were prepared in accordance with the following general sequence:

1) Mechanical polishing with 1200 and 2400 grit paper;

2) Rinsed with bidistilled water, degreased ultrasonically in ethanol before use and dried at room temperature.

3) Immersion in chitosan solution.

2.3. Instrumentation

The measurements were carried out with a potentiostat/galvanostat. EIS measurements were done using Autolab PGSTAT 73022 at an open circuit potential with applied 10 mV sinusoidal perturbations in the 100 kHz to 0.1 mHz frequency range, taking 7 steps per decade was used. For this purpose, a conventional three-electrode cell was used, composed of Ag/AgCl reference electrode, a platinum wire as the counter electrode, and the chitosan-coated mild steel substrates as the working electrodes. All the measurements were done in a Fara-day cage in order to avoid electromagnetic

interference and the impedance plots were fitted using FRA software. Cathodic and anodic polarization curves were scanned from -0.1 V to -0.8 V with a scan rate of 1 mV s^{-1}. EPD was performed using a DC, MSC, Power supply.

Scanning electron microscopy (SEM) (Philips, XI 30) was used for characterization of the homogeneity of the coatings; the samples were coated with gold before SEM examination. While FTIR, (Bruker Instruments, Germany) was used to determine the chemical groups in the wavenumber region 4000–500 cm^{-1}.

3. RESULTS AND DISCUSSION

3.1. Surface and film morphologies

Fig. 2 shows the surface morphology of freshly prepared chitosan coated mild steel with two magnifications produced by EPD before being immersed in 0.5 M H_2SO_4. Transparent, homogeneous chitosan film was noticed. The coatings were seen to be flexible and exhibited qualitative good adherence to the substrate. The experiments confirmed that EPD technique forms a good adherent CS film. The EPD mechanism of chitosan macromolecules has been explained by Zhitomirsky and co-workers [16]. Chitosan macromolecules are protonated in the aqueous solution to form poycation. During the EPD process, electrolysis of water occurs that increases the local pH at the cathode consequently, the protonated amine-groups of chitosan lose their charge at the cathode surface to form an insoluble deposit. In solution, the charge of chitosan depends on its molecular weight and deacetylation degree (DA) as well as on negatively charged counter ions [17].

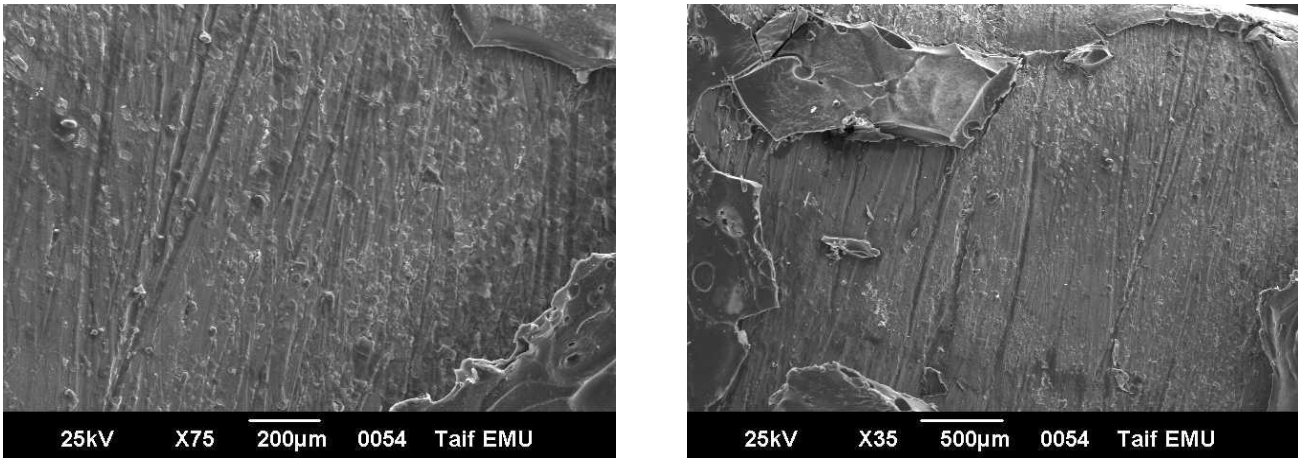

A **B**

Figure 2. (a) SEM micrographs showing the surface of CS films fabricated by EPD with electrical field 15 V/cm. (Deposition time = 15 min) over mild steel (magnification 200 and 500 μm).

Fig. 3(a,b) is the surface morphology of uncoated mild steel (blank), and chitosan coated steel, respectively, after immersion in 0.5M H_2SO_4 solution for 48 hours with two magnifications. It was found that for the blank corrosion products could be observed in Fig. 3a which are like metal hydroxides and oxides [18].

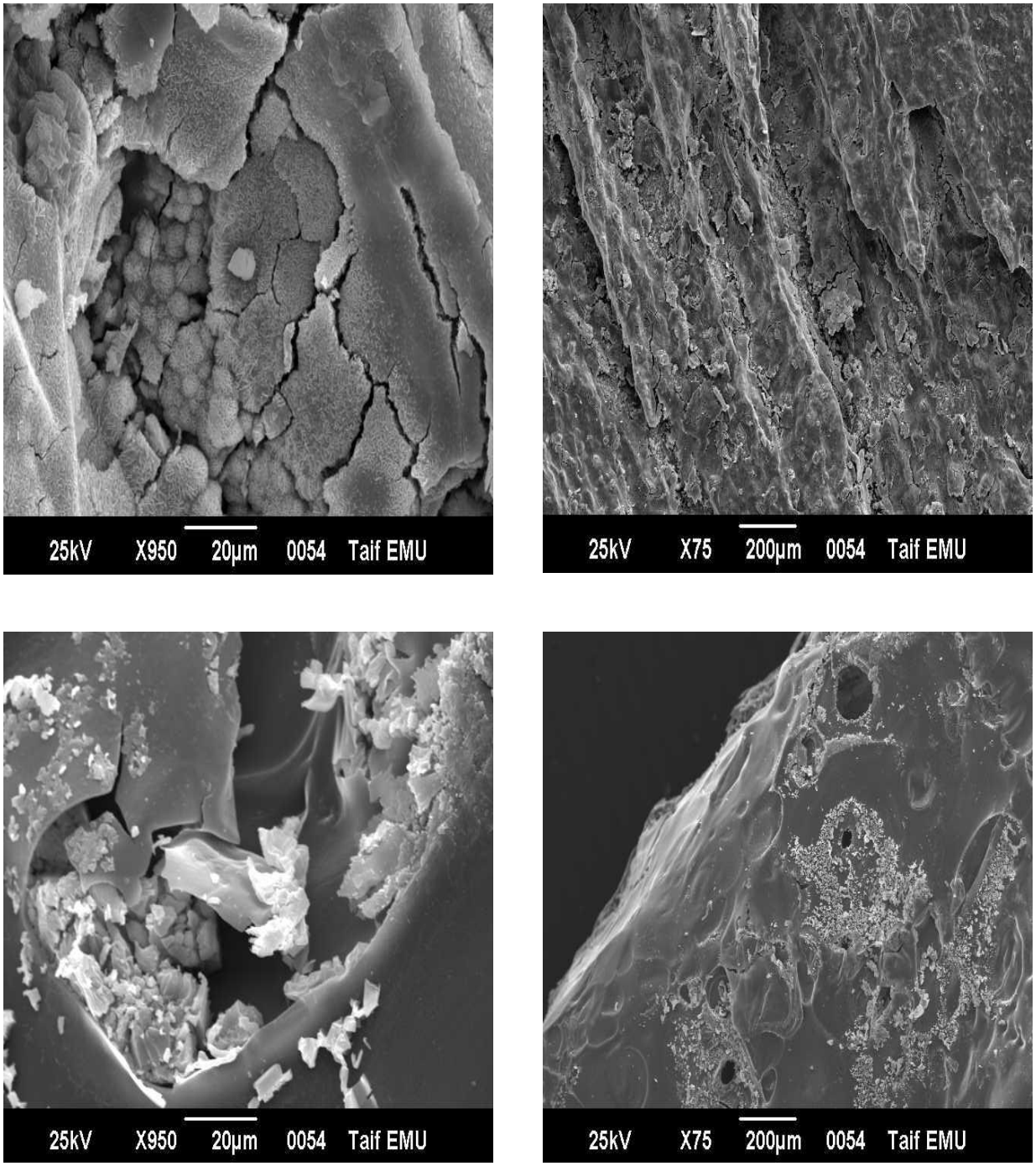

Figure 3. SEM micrographs of (a) uncoated mild steel electrode, (b) CS coated mild steel after immersion for (48 h) in 0.5 M H_2SO_4 solution, at 298 K (magnification 20 and 200 μm).

Fig. 3a shows a lot of cracks on the surface like a net. However, for chitosan coated alloy (Fig. 3b), it is apparent that the synthesized polymer films had a structure significantly different from that of the blank showing flowery structure at lower magnification with almost no corrosion products on the surface, its morphology is quite different such that the image is much more smooth than the blank showing that the substrate is more protected. It shows almost 100% coverage of the metal surface by inhibitor molecules. Thus minimum corrosion occurs at this concentration and hence corrosion is inhibited strongly in acid media.

3.2. FTIR spectroscopy investigation of possible mechanism for glutaraldehyde cross-linking to chitosan

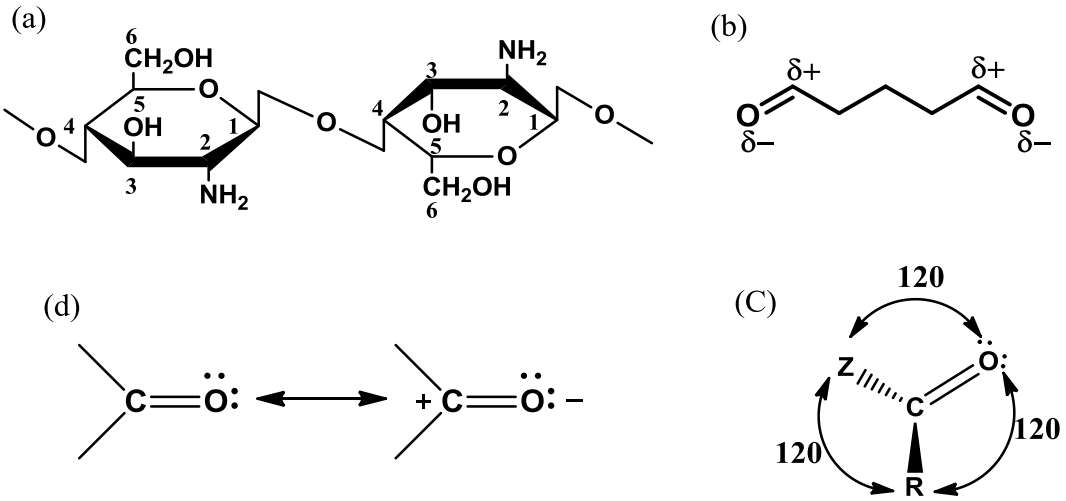

Figure 4. Possible reaction routs for glutaraldehyde cross-linking to CS fiber. (a) CS, (b) glutaraldehyde, (c) Carbonyl, (d) Resonance structure for the carbonyl group.

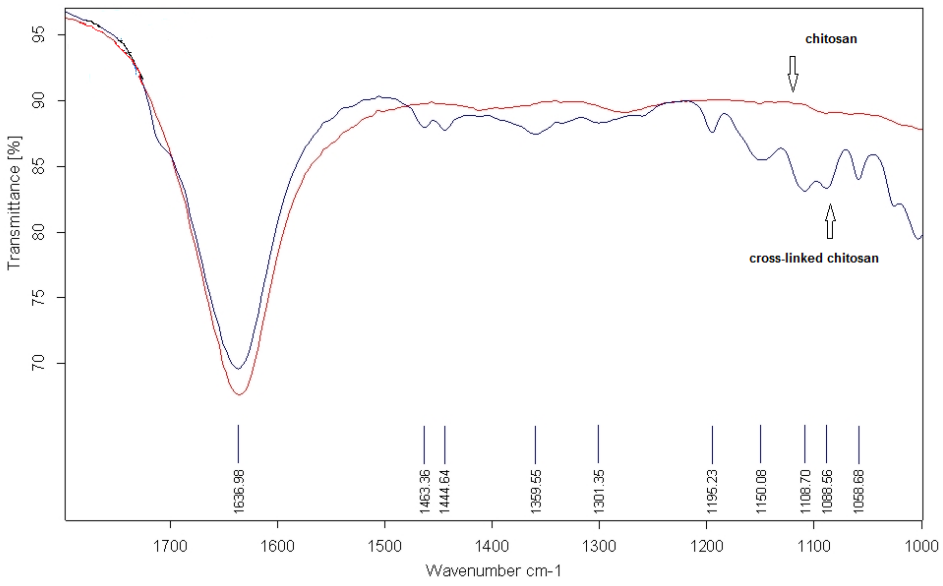

Figure 5. FTIR spectrum of a CS before and after cross-linking with glutaraldehyde.

Considering the halobiosic chitosan has a structure with two hydroxyl groups and an amino group in one glucosamine ring (Fig. 4(a)), and the glutaraldehyde molecule has two carbonyl groups (Fig. 4(b)), especially the carbon of carbonyl groups due to located in sp^2 easily hybridized to cause attachment from other three atoms lying in the same plane to yield the bond angles among these three atoms to form a trigonal coplanar structure, e.g. approximately 120° (Fig. 4(c)). Moreover, the carbonyl carbon and carbonyl oxygen are available to present several positive and negative charges influenced by the electronegative oxygen and the resonance contribution of the second structure (Fig. 4(d)). To observe these evidences and understand the mechanism for glutaraldehyde cross-link with chitosan, FTIR spectra for chitosan before and after crosslinking were presented in Fig. 5. It shows new peaks appeared for chitosan after crosslinking reaction indicating that glutaraldehyde have reacted with the hydroxyls of the glucosamine rings due to acetalization and in good agreement with other studies [19]. According to Solomons, dissolution of aldehyde in alcohol can yield hemiacetal by nucleophilic addition of the alcohol to the carbonyl group, and this process has a basic feature on hemiacetal, i.e. its –OH and –OR groups to be attached by the same carbon atom. Based on above discussion, the possible mechanism for glutaraldehyde cross-linked to chitosan was furthermore outlined in Fig. 6.

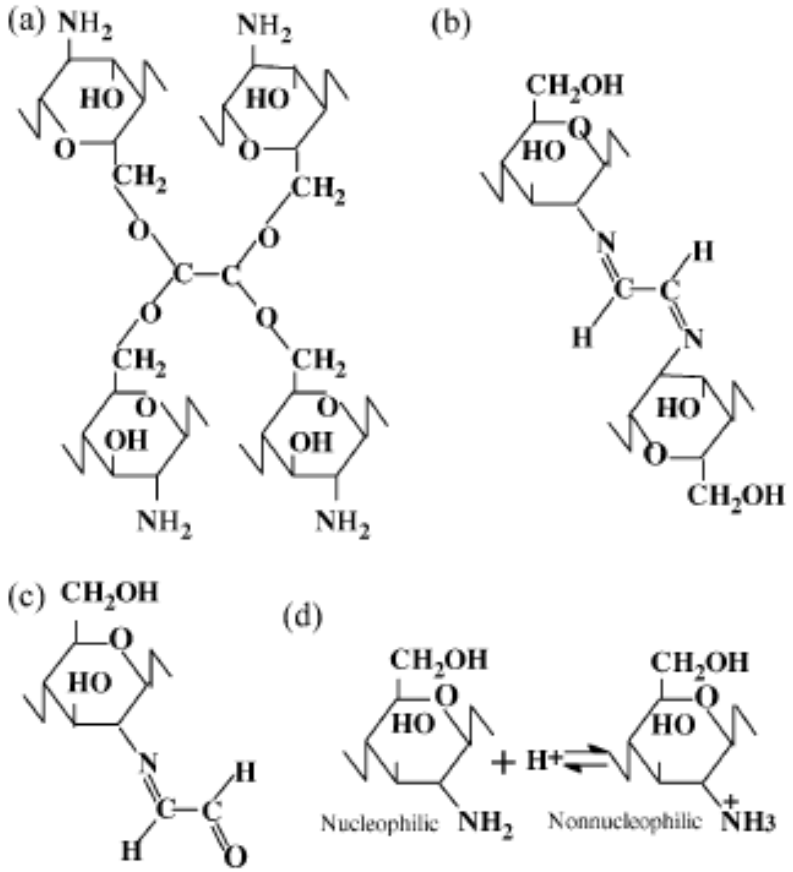

Figure 6. Mechanism for glutaraldehyde cross-linking to CS. Glutaraldehyde reaction with a) hydroxyl groups, b) amino groups in CS, c) one carbonyl in a glutaraldehyde reacts, (d) Effect of acid on CS nucleophilicity.

3.3. FTIR spectroscopy investigation of adherence of chitosan film

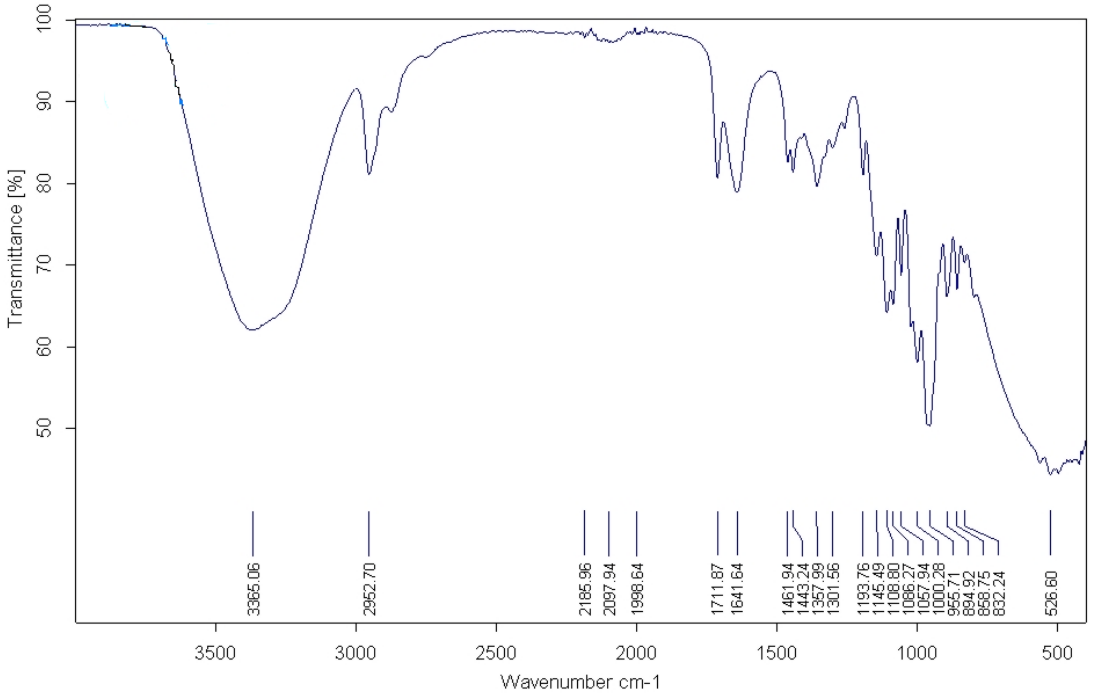

Figure 7. FTIR spectrum of a CS film deposited on mild steel by EPD (EPD conditions: E = 15 V/cm, t = 15 min).

FTIR spectroscopy was used also to determine the chemical groups in the films, in order to verify the presence of chitosan on the substrate and to check that the deposited chitosan layer was not degraded during the deposition process. A typical FTIR spectrum of chitosan coating is shown in Fig. 7. The peaks around 894 cm^{-1} and 1145 cm^{-1} correspond to the saccharide structure. They are caused by the vibrations of the glycosidic bonding (-C-O-C-) which occurs between the repeating unit from chitosan [20–22]. The peak at 1641 cm^{-1} corresponds to the amide I band. This signal is caused by stretching of the C-O group in the glucosamine unit [21, 22]. The amide II band at 1460 cm^{-1} corresponds to the NH-bending vibrations in the amide group [21, 23]. The peak at 1357 cm^{-1} hints at the so-called amide III band. This peak is caused by linked C-H-N-H deformation vibration. The broad peak at 3365 cm^{-1} is caused by two different processes: on one hand the peak hint to N-H symmetrical vibrations, on the other hand it indicates vibrations of hydroxyl groups [20, 21].

3.3. EIS measurements

3.3.1. Effect of CS polymer film

Fig. 8 shows the impedance spectra measured at the open circuit potential for uncoated and chitosan coated samples (EPD parameters: E = 15 V/cm, t = 15 min) exposed to 0.5 M H_2SO_4 at 298 K after immersion for 48 hour. The bare mild steel shows the expected passive behavior in the acidic solution with low values of impedance at low frequencies. The coated mild steel with

electrophoretically deposited chitosan (E = 15 V/cm, t = 15 min) shows higher values of impedance at low frequencies. Also uncoated alloy shows maximum phase angle to be nearly 20°, however for coated electrode a phase angle maximum reaches to 58°, suggesting a higher corrosion resistance than the bare mild steel sample. This is not surprising as the chitosan coating acts as an additional barrier.

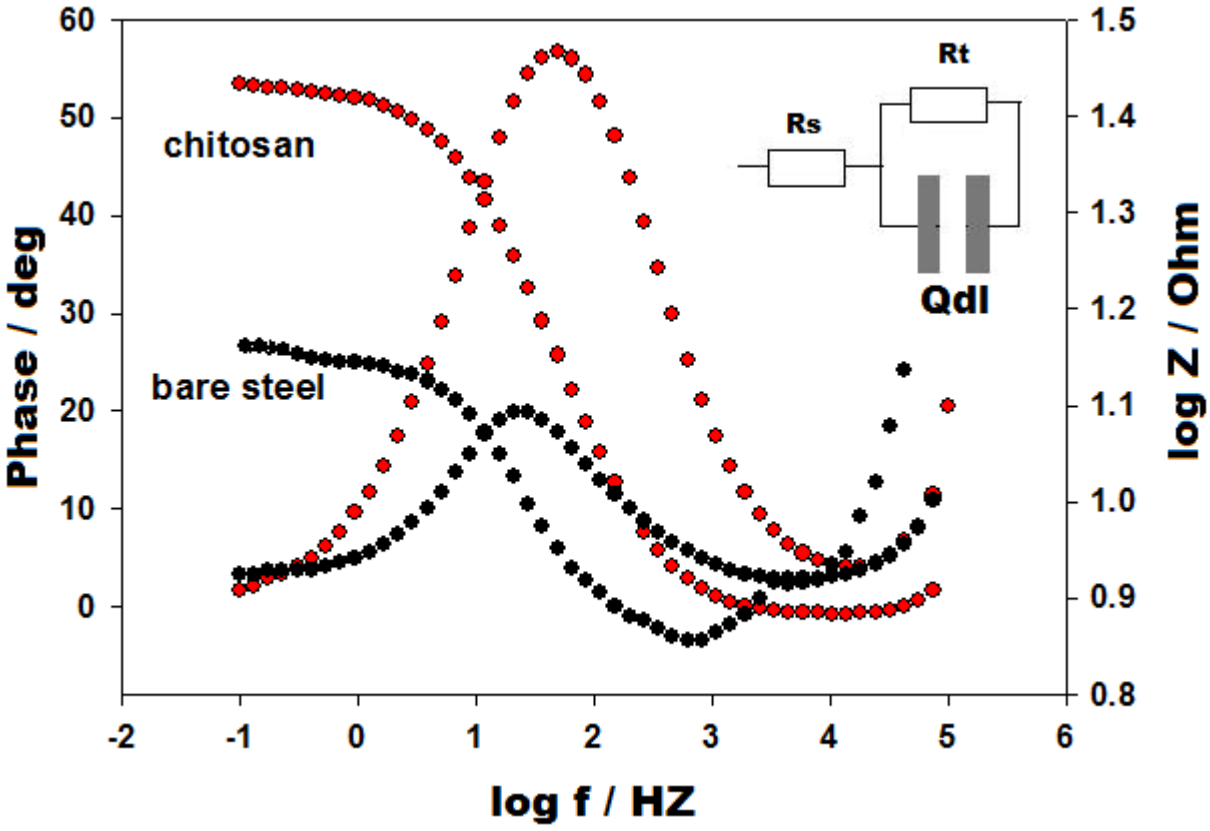

Figure 8. Bode plots of steel with and without CS in 0.5 M H_2SO_4 solution for 48 hours immersion at 298K, and equivalent circuit model representing one time constant inserted in it.

The experimental EIS diagrams in Fig. 8, show that log|Z| tends to become constant at high frequencies, with the phase angle values falling towards zero with increasing frequency. Although the electrochemical impedance was measured down to very low frequencies (100 mHz), the Bode plots show a resistive region (horizontal line and a phase angle θ~0) at these frequencies. Bode plots show that phase angle is greater for CS coated steel compared to uncoated steel. This is related to the resistance of coating against penetration of corrosive sulfuric acid medium. Computer simulation of the EIS results was performed using a complex non-linear least-square (CNLS) fitting procedure in order to establish which electrical equivalent circuit (EEC) best fits the experimentally obtained impedance data. Using a constant phase element (CPE) [24], the simple Randle's equivalent circuit was found to be satisfactory for fitting the impedance data. The model (inserted in Fig. 8) consisted of a solution resistance (Rs) in series with RC parallel combination of (R_t/Q_{dl}) which represents the oxide film resistance and a constant phase element (CPE) instead of an ideal capacitance element for the oxide film, respectively [24]. In case of solid materials, the usage of CPE is to describe the non-

homogeneities in the system. The R_t values refer to charge transfer resistance of the steel/electrolyte interface and the CS coating resistance. The impedance associated with the capacitances of the oxide layers is described by the complex frequency dependent impedance (Z_{CPE}) defined as [24]:

$$Z_{CPE} = [Q(j\omega)^{\alpha}]^{-1} \quad (1)$$

Q is the frequency independent constant, j^2 is −1 and ω is the angular frequency. α Values are the correlation coefficients for the CPE ($0 < \alpha < 1$). The impedance parameters obtained for CS coated steel in 0.5M H_2SO_4 solution are given in Table 1. R_t and Q_{dl} jointly belong to the electrochemistry of corrosion at the polymer–metal interphase after coating penetration by corrosive anions [25–28]. Effective corrosion resistance is associated with high R_t and low Q_{dl} values [25–28]. As can also be seen in Table 1, R_t value of CS coated mild steel is higher than those of the uncoated steel, since the penetration on electrode surface of corrosive acidic medium is inhibited by conducting polymer coating. The Q_{dl} value of CS coated steel is lower than those of the uncoated steel due to inhibition of electron transfer to polymer from metal indicating higher relative thickness of coated steel. These results show protective property of the coating. The corrosion resistance of coated CS on electrochemically mild steel surfaces is due to homogeneous polymer coated surface, stability of electroactivity and/or high conductivity of coatings and occurrence of a homogeneous polymer/metal interphase during electrosynthesis [29].

Table 1. Polarization and impedance parameters for uncoated and CS-coated mild steel in 0.5 M H_2SO4.

electrode	R_t (Ω cm^2)	Q_{dl} ($\mu F cm^{-2}$)	α	R_s (Ωcm^2)	i_{corr} ($\mu A cm^{-2}$)	E_{corr} mV	IE% Tafel
Uncoated Mild steel	45.0	129	0.77	1.2	600	-367	
CS coated Mild steel	130	103	0.92	0.8	11	-273	98.1

3.3.2. Effect of immersion time

The corrosion behavior for uncoated and chitosan coated samples (EPD parameters: E = 15 V/cm, t = 15 min) exposed to 0.5 M H_2SO_4 at 298 K with immersion time for 2 days is studied and shown in Fig. 9 as Nyquist plots. The diameter of the depressed circles increases slowly with increasing immersion which suggests that the formed surface film remains stable for time of immersion reaches to more than 48 hours. Also, this indicates that a charge transfer process mainly controlling the corrosion of mild steel. Such behavior is characteristic for solid electrodes and often refers to frequency dispersion, has been attributed to roughness and other in homogeneities of the solid surface. This may be related to slow transformation of partly oxidized form of film to reduced form that is stability of the oxidation states [30]. However, for bare mild steel, the corrosion increases and

the diameter of the circuit decrease. Therefore, CS coating on mild steel surface offers good corrosion protection in a 0.5 M sulfuric acid medium for 48 hours.

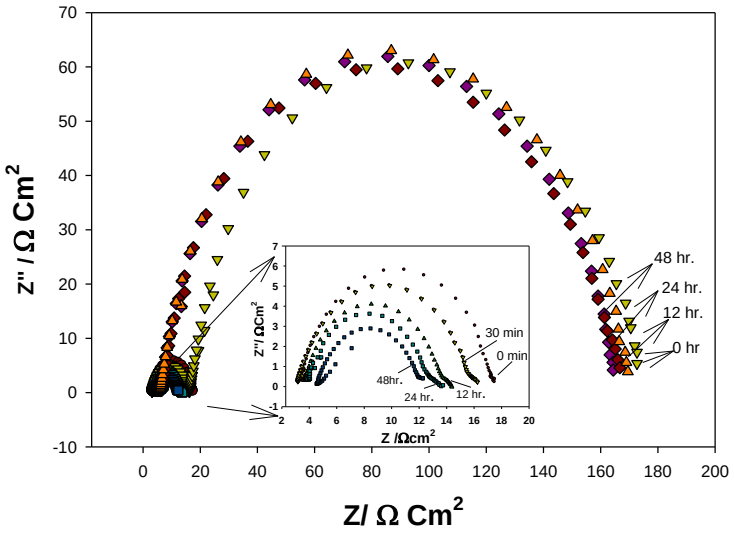

Figure 9. Nyquist plots in 0.5 M H_2SO_4 solution, at different immersion times for CS coated mild steel, and bare mild steel (inset)

This can also be explained by some decrease of the surface heterogeneity, due to the adsorption of the CS molecules on the most active adsorption sites. Thus corrosion action decreases with increasing time of immersion till 48 hours.

3.4. Potentiodynamic polarization measurements

The anodic and cathodic (E-log i) plots (Fig. 10) of coated and uncoated mild steel alloy in 0.5 M sulfuric acid were studied using Potentiodynamic polarization measurements at a scan rate of 1.0 mV s^{-1}. The curves were swept from –0.1 V to -0.8 V vs. SCE. Prior to the potential scan the electrode was left under open circuit conditions in the respective solution for 48 hours. Polarization parameters are listed in Table 1. The polarization curves showed a clear difference between the uncoated and coated mild steel alloy. The corrosion potentials (E_{corr}) of the coatings chitosan on mild steel substrate were shifted by 132–164 mV toward more negative potentials, indicating a porous film formed on the surface. Furthermore, it was observed that the corrosion current density (I_{corr}) of the chitosan coating was more than three orders of magnitude lower than that uncoated steel alloy, confirming that the chitosan coating on mild steel alloy promoted its corrosion resistance. This indicates a higher corrosion resistance of the coatings [21] and by calculating the inhibition efficiency using the following equation:

$$IE\,\% = \frac{i^{\circ}_{corr} - i_{corr}}{i^{\circ}_{corr}} \,\mathrm{X}\, 100 \qquad (2)$$

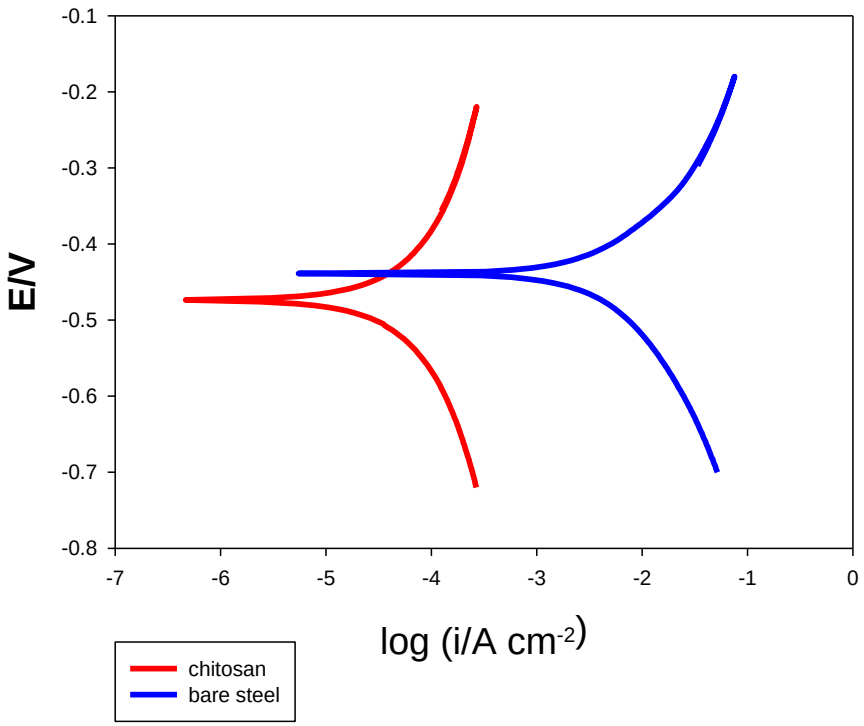

Figure 10. Potentiodynamic polarization scans of both uncoated and coated mild steel alloy in 0.5 M H_2SO_4 after 48 hours immersion at 298K.

CS provides protection of about 98.1% in corrosive medium. Finally, from the polarization curves, it was found that the coating formed on the mild steel alloy significantly promoted its resistance to corrosive degradation. Generally all results using different techniques confirm each other.

4. CONCLUSIONS

- It is possible to produce adhesive chitosan films on mild steel by EPD method. Chitosan coating structure was demonstrated by FTIR. SEM indicates the presence of the chitosan layer with good corrosion inhibition of the coated mild steel.
- This study indicated that the mechanical properties of chitosan could be enhanced using glutaraldehyde as reagent and cross linker. Based on IR spectra the cross-linking method was described between chitosan and glutaraldehyde.
- Potentiodynamic polarization curves and electrochemical impedance spectroscopy results showed a better corrosion behavior of chitosan coated substrates in 0.5 M H_2SO_4 at 298 k with respect to bare mild steel. Good inhibition efficiency (IE) has been found in 0.5 M sulphuric acid solution reaches to 98.1%.

ACKNOWLEDGMENTS
We gratefully acknowledge chemistry department (University of Taif, kingdom of Saudi Arabia) for financial support to carry out the above investigations. We thank Dr. Sahar Faddlallah for her comments and supports.

References

1. M. El Achouri, M.R. Infante, F. Izquierdo, S. Kertit, H.M. Gouttoya, B. Nciri, *Corros. Sci*. 43 (2001) 19.
2. A.M. Fekry, R.R. Mohamed, *Electrochim. Acta* 55 (2010) 1933.
3. S.S. Abd El Rehim, M.A.M. Ibrahim, K.F. Khalid, *J. Appl. Electrochem*.29 (1999) 593.
4. J.M. Sykes, *Br. Corros. J*. 25 (1990) 175.
5. S. Rengamani, S. Muralidharan, M. Anbu Kulamdainathan, S. Venkatakrishna Iyer, *J. Appl. Electrochem*. 24 (1994) 355.
6. M. Ajmal, A.S. Mideen, M.A. Quraishi, *Corros. Sci*. 36 (1994) 79.
7. A.El-Sayed, *J. Appl. Electrochem*. 27 (1997) 193.
8. J. Sinko, *Prog. Org. Coat*. 42 (2001) 267.
9. S.E. Manahan, Environmental Chemistry, sixth ed. Lewis, Boca Raton, 1996.
10. S. Hiano, H. Inui, H. Kosaki, Y. Uno, T. Toda, in: C.G. Gebelein, C.E. Carraher Jr. (Eds.), Biotechnology and Bioactive Polymers, Plenum Press, New York, 1994, p. 43.
11. Gabrielii, P. Gtenholm, *Proc. ACS Div. Polym. Mater.* 79 (1998) 459.
12. P.A. Sandford, A. Steinners, in: S.W. Shalaby, C.L. McCormick, G.B. Butles (Eds.), Water-soluble Polymers, ACS Symposium Series 467, Washington, DC, 1991, p. 430.
13. A.R. Boccaccini, S. Keim, R. Ma, Y. Li, I. Zhitomirsky. *J. R. Soc. Interface* 7 (2010) 581.
14. A.R. Boccaccini, I. Zhitomirsky. *Curr. Opin. Solid State Mater. Sci.* 6 (2002) 251.
15. L. Besra, M. Liu. *Prog. Mater. Sci*. 52 (2007) 1.
16. I. Zhitomirsky, A. Hashambhoy. *J. Mater. Process Technol*. 191 (2007) 68.
17. O.V. Bobreshova, O.V. Bobylkina, P.I. Kulintsov, G.A. Bobrinskaya, V.P. Varlamov, S.V. Nemtsev. *Russ J. Electrochem*. 40 (2004) 694.
18. K. Bhrara, H. Kim, G. Singh, *Corros. Sci*. 50 (2008) 2747.
19. Solomons, T. W. G. (1980). Organic chemical. New York: Wiley (pp. 703–714).
20. A. Pawlak, M. Mucha. *Thermochim. Acta* 396 (2003) 66.
21. De Souza CJE, Pereira MM, Mansur HS. *J. Mater. Sci. Mater Med* 20 (2009)61.
22. J. Kumirska, M. Czerwicka, Z. Kaczyński, A. Bychowska, K. Brzozowski, J. Thöming, et al. *Mar. Drugs* 8 (2010) 636.
23. F. Sun, X. Pang, I. Zhitomirsky. *J. Mater. Process Technol.* 209 (2009) 606
24. A.M. Fekry, Electrochim. Acta 54 (2009) 3480.
25. S.L.A. Maranhao, I.C. Guedes, F.J. Anaissi, H.E. Toma, I.V. Aoki, *Electrochim. Acta* 52 (2006) 519.
26. N.V. Krstajic, B.N. Grgur, S.M. Jovanovic, V. Vojnovic, *Electrochim. Acta* 42 (1997) 1685.
27. G. Kousik, S. Pitchumani, N.G. Renganathan, *Prog. Org. Coat.* 43 (2001) 286.
28. P. Li, T.C. Tan, J.Y. Lee, *Synth. Met.* 33 (1998) 20.
29. Ya˘gan, N.O. Pekmez, A. Yıldız, *Corros. Sci.* 49 (2007) 2905.
30. Ya˘gan, N.O. Pekmez, A. Yıldız, *Electrochim. Acta* 53 (2008) 2474.